Sumalay Roy, Katayoon Mohseni, Stefan Förster, Martin Trautmann, Florian Schumann, Eva Zollner, Holger Meyerheim* and Wolf Widdra

The Kepler tiling as the oldest complex surface structure in history: X-ray structure analysis of a two-dimensional oxide quasicrystal approximant

DOI 10.1515/zkri-2016-2004
Received September 12, 2016; accepted October 16, 2016; published online November 16, 2016

Abstract: We have carried out a surface X-ray diffraction (SXRD) analysis of the approximant structure related to the recently discovered two-dimensional dodecagonal oxidic quasicrystal. The structure is characterized by the $3^2.4.3.4$ Archimedean tiling, first described by Kepler in 1619. The tiling network is related to titanium atoms observed as protrusions in scanning tunneling microscopy images. All four titanium atoms within one two-dimensional unit cell ($a_0 = 13.1$ Å, $b_0 = 12.9$ Å, $\gamma = 90.5°$) are surrounded by three oxygen atoms. The TiO_3 units are separated by barium atoms. The total stoichiometry is given by $Ba_4\ Ti_4\ O_{10}$.

Keywords: approximant; Archimedean tiling; barium titanate; oxidic quasicrystal; surface X-ray diffraction.

Quasicrystals (QCs) represent an unusual state of matter. While they posses long-range order giving rise to sharp diffraction spots, they lack lattice periodicity. Since their discovery in 1984 [1] numerous studies have concentrated on the synthesis, structural characterization and physical properties of QCs. An overview is given in Ref. [2]. QCs investigated in the past where primarily composed of intermetallic alloys [1, 3] and soft materials [4–6]. Only recently, an oxide derived QC (OQC) has been discovered [7]. The OQC was prepared by sputter deposition of an ultra-thin film of perovskite type barium titanate ($BaTiO_3$) on the (111) surface of Pt followed by annealing in ultra-high vacuum at 1150 K [7]. The OQC was unambiguously identified by low-energy electron diffraction (LEED) and scanning tunneling microscopy (STM) images.

It is well known that for a given QC phase in many cases one or several approximants can exist, which are characterized by periodic lattices, but bear many resemblances to the QC structure such as the presence of common building blocks [8]. In the $BaTiO_3$/Pt(111) OQC system, the approximant forms if the annealing temperature is increased to approximately 1250 K. The approximant to the OQC corresponds to the $3^2.4.3.4$ Archimedean tiling which was already discussed by Kepler in 1619 [9, 10]. Figure 1a and b compare the STM images of the OQC and its approximant, respectively. The two tilings which are identified by the apparent protrusions in the STM images are characterized by arrangements of triangles, squares and 30° rhombs. The latter occurs only for the OQC as emphasized in Figure 1a. In the case of the OQC, the tiling corresponds to the the Stampfli–Gähler tiling [12, 13]. The red square in Figure 1b represents the unit cell of the approximant. It is characterized by an almost quadratic two-dimensional unit cell (plane group *p2*) with lattice parameters $a_0 = 13.1$ Å, $b_0 = 12.9$ Å, and $\gamma = 90.5°$. It is related to the (1×1) unit cell of the Pt(111) substrate by the transformation matrix ($a_{11} = 27/5$; $a_{21} = 2$; $a_{21} = 3/4$; $a_{22} = 5$). We note that this is the unit cell used in the surface X-ray diffraction (SXRD) analysis and emphasize that it represents a projection of a 20 times larger unit cell with transformation matrix ($a_{11} = 27$; $a_{21} = 10$; $a_{21} = 3$; $a_{22} = 20$). This large unit cell is the crystallographically correct one if the Moiré modulation of the structure with periodicity 2.78 nm is taken into account. The Moiré modulation of the structure is nicely seen in the 17×17 nm^2 STM image in Figure 1c where the 2.8 nm periodicity is highlighted be the black lines. The arrow which is orthogonally oriented indicates the modulation vector which encloses an angle of approx. 32° with the a-axis of the small unit cell.

Since the characteristic distance between the protrusions equals to approximately 6.7 Å in both structures it has already been assumed that they represent one sublattice of the structures, but an unambiguous assignment to

***Corresponding author: Holger Meyerheim,** Max-Planck-Institut f. Mikrostrukturphysik, Weinberg, 2, D-06120 Halle, Germany, E-mail: hmeyerhm@mpi-halle.mpg.de
Sumalay Roy and Katayoon Mohseni: Max-Planck-Institut f. Mikrostrukturphysik, Weinberg, 2, D-06120, Halle, Germany
Stefan Förster, Martin Trautmann, Florian Schumann, Eva Zollner and Wolf Widdra: Institut für Physik, Von Danckelmann Platz, 3, D-06120 Halle, Germany

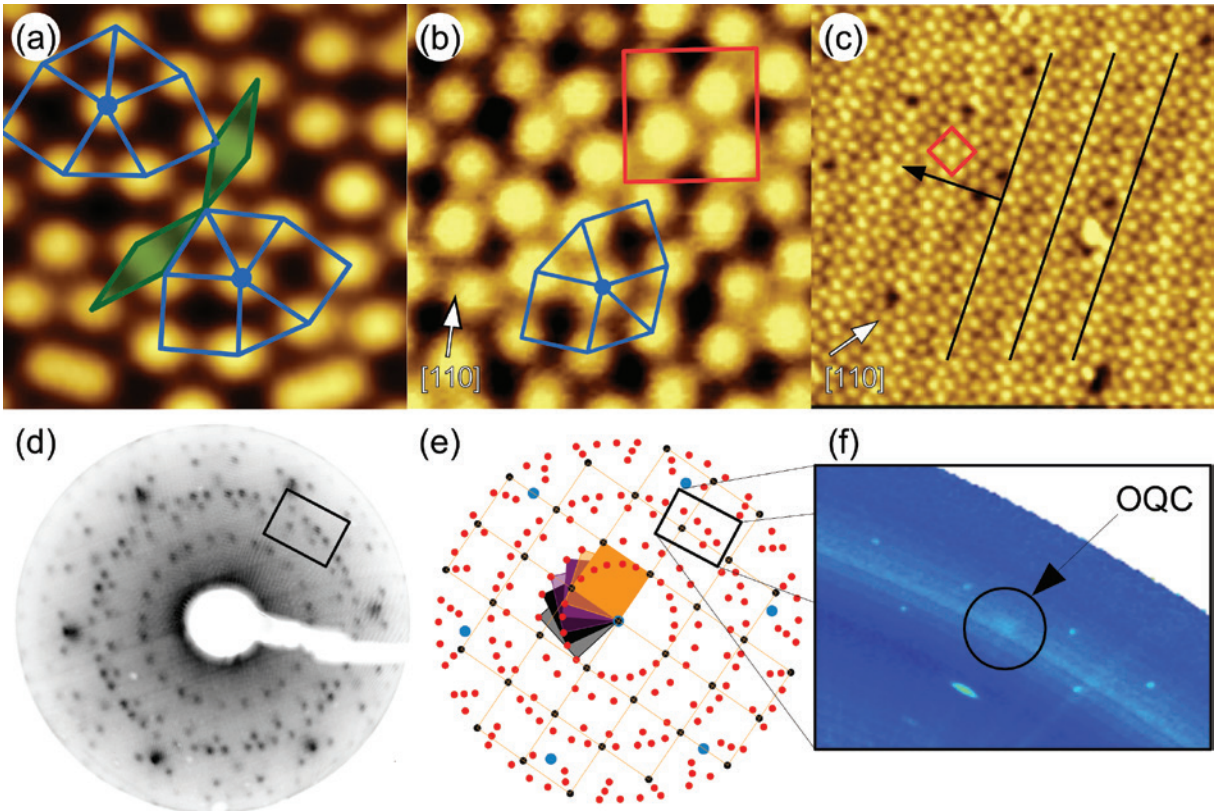

Fig. 1: Scanning tunneling microscopy images of the OQC (a) and its approximant (b). STM parameters for OQC = 4 × 4 nm², I = 0.3 nA, U = 1.0 V, for approximant = 3.5 × 3.5 nm², I = 30 pA, U = 0.1 V). The building bloc of the Kepler tiling common to both structures is emphasized. In (a) the rhombs which occur only in the OQC structure are highlighted. The red square in (b) emphasizes the unit cell used for the structure analysis. (c): Large scale (17 × 17 nm², I = 0.5 nA, U = – 1.0 V) STM image showing the 2.78 nm modulation periodicity (emphasized by black lines) oriented 30° relative to the unit cell (red square). The arrow indicates the modulation direction. (d): Experimental (E = 20 eV) and schematic (d) LEED pattern of the approximant highlighting the orientation of the six domains (colored squares represent unit cells in reciprocal space of different domains. Large (blue) dark spots represent first order reflections of the Pt(111) surface (see also Ref. [11]). (f): X-ray diffraction spots of the approximant and of the OQC (black circle) within the black rectangle in (d) and (e) collected at $\ell \approx 0$.

one atomic species (e.g. barium or titanium) has not been possible so far. In Ref. [7] it was suggested the tunneling involving titanium d-orbitals is responsible for the STM contrast, but this view was challenged by a recent study [14] which proposed barium atoms forming the Stampfli–Gähler tiling.

The X-ray analysis of the OQC structure by the classic methods as described for instance in Ref. [2] is difficult. This is because of the limited amount of reflections intense enough to be collected even by using highly brilliant synchrotron X-ray sources such as provided by the European Synchrotron Radiation Facility (ESRF) in Grenoble (France). However, due to the similarity of the OQC structure with its approximant, the structure analysis of the latter provides information about the major building blocks of the OQC as highlighted in Figure 1a and b. In this study we provide a complete analysis of the approximant structure using SXRD. In a previous publication [11] it was shown that the Kepler tiling is formed by titanium atoms which are surrounded by three oxygen atoms each. Barium atoms are located approximately at the edges of the tiling elements. Here, we present important details of the atomic structure and how the model was derived by starting with a model free analysis of the reflection intensities based on the projected Patterson function [P(u, v)]. We emphasize that the OQC approximant structure is purely two-dimensional, i.e. the third coordinate in reciprocal space, ℓ, is a continuous parameter. Our analysis represents one of the very few examples of an application of the classical Fourier techniques to solve a surface structure.

The preparation of the approximant structure was carried out as outlined in Ref. [11] using the UHV diffractometer at the ID03 beamline of the ESRF where the experiments have been performed. During preparation the (270) reflection was monitored versus time to optimize

the area fraction of the approximant structure on the Pt(111) surface. The formation of the approximant is also identified by LEED images, one of which is shown in Figure 1d collected at an energy of 20 eV. It is compared with a schematic in Figure 1e clarifying the domain structure on the Pt(111) surface. In total, three 120° rotated structures with two mirror domains exist as indicated by the different squares representing the unit cell is the approximant structure in reciprocal space. In total, the integrated intensities of 176 reflections of type (hk0) were collected using a 2D pixel detector under total reflection conditions of the incident beam ($\lambda = 1.1$ Å). We note that due to the large number of domains, the large unit cell and the majority of atoms having small scattering amplitudes, reflection intensities are very low in general, orders of magnitude weaker than typical crystal truncation rod intensities [15]. Figure 1f shows several approximant and one OQC X-ray reflection, the latter indicated by the black circle. Reflections in (f) correspond to spots in the black rectangles in (d) and (e). It can be seen that the approximant reflections are relatively sharp as compared to that of the OQC which forms the minority phase under the given preparation conditions.

After averaging over symmetry equivalent reflections and reflections of equivalent domains, 43 symmetry independent reflections were used for the structure analysis. Structure factor amplitudes ($|F_{obs}$ (hk0)|) of equivalent reflections agree to within about 15% which can serve as an estimate of the total standard deviation. We emphasize that for the refinement no weighting scheme was used and the un-weighted residuum (R_U) [16] serves as the parameter of the fit quality. The approximant structure can be viewed as an almost perfect 2D one, in that it is only composed of a single layer of barium, titanium and oxygen atoms located at almost the same level.

The data analysis was carried out by exploiting the classical Fourier transformation (FT) methods originally developed for 3D crystallography (for more details see Ref. [17]), here applied to the 2D case. Based on 43 independent reflections with structure factor amplitudes of type $|F_{obs}(hk0)|$ the 2D *(z-projected)* Patterson function, P(u, v), was calculated given by: $P(u, v) = \sum |F_{obs}(hk0)|^2 \times \cos 2\pi(hu + kv)$. The summation runs over all reflections (hk0). Peaks in P(u, v) represent interatomic vectors whose heights are proportional to the atomic numbers (Z_i, Z_j) of the respective species (i, j) and the multiplicity (M) of their occurrence within the unit cell, i.e. $P(u, v) \propto Z_i \times Z_j \times M$ [17]. In general, difficulties in the interpretation of P(u, v) may arise by the interference between nearby vectors, but in many cases a first guess of basic features of the structure is possible, especially in the present case where it contains heavy barium atoms, which dominate the total scattered amplitude.

In Figure 2 we compare P(u, v) (a) with the best fit model of the structure (b). The refined atomic coordinates are listed in Table 1. Apart from the trivial maximum at the origin ($\vec{R} = 0$) corresponding to the self-correlation of all atoms, several symmetrically independent peaks appear within the asymmetric unit ($u \in [0, \frac{1}{2}]$, $v \in [0, 1]$). In Figure 2a some peaks are labeled by (A), (B) (C) and (D) together with the vectors which are directly transferred to Figure 2b for comparison. It is possible to relate the peaks to correlations between atoms. For instance, the strong peak (A) can be attributed to an interatomic vector between atoms Ba(1) and Ba(3). Also, the weaker peaks (C) and (D) can be correlated to O–O interatomic vectors. The first one has a high multiplicity M = 4 related to the vector (green) between atoms O(6) and O(8) as well as between

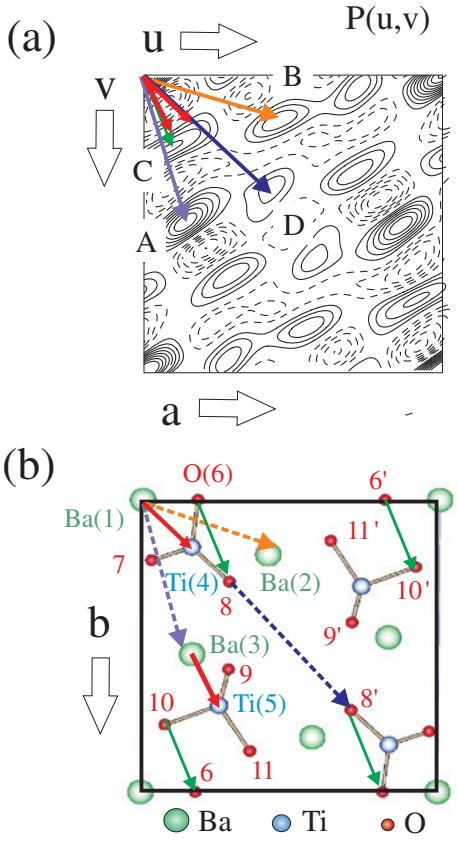

Fig. 2: (a): 2D Patterson function of the approximant structure. Positive peaks (solid lines) are related to interatomic vectors as shown. (b): Structure model for the approximant based on the least squares refined structure factor amplitudes. Green, blue and red spheres correspond to barium, titanium and oxygen atoms, respectively. Labels 1–11 correspond to atoms listed in Table 1. Some interatomic vectors are shown and compared with the corresponding peaks in P(u, v) in (a).

Tab. 1: Structure parameters of the approximant based on the best fit. Parameters *x* and *y* represent coordinates within the unit cell (a_0 = 13.1 Å, b_0 = 12.9 Å and γ = 90.5°, plane group symmetry *p2*). Labels (1) to (11) refer to atoms in Figures 2–4. The parameter Θ indicates the site occupancy. Parameters U_{iso} and U_{ij} represent static mean squared displacement amplitudes in the case of isotropic and anisotropic refinement, respectively (standard deviation about 50%. Standard deviations for *x* and *y* are approximately equal to ± 0.01 for the barium and titanium positions and ± 0.02 – 0.04 for the oxygen positions, respectively. Uncertainties for the Us are 30% at most.

Number	Species	Θ	*X*	*y*	U_{iso} (Å²)	U_{11}	U_{22}	U_{12}
(1)	Ba	1.0	0.000	0.000	0.28	0.88	0.65	– 0.57
(2)	Ba	0.5	0.423	0.187	0.09	0.67	0.40	– 0.28
(3)	Ba	1.0	0.170	0.529	0.28			
(4)	Ti	1.0	0.165	0.162	0.02			
(5)	Ti	1.0	0.262	0.703	0.02			
(6)	O	1.0	0.185	0.000	0.05			
(7)	O	1.0	0.030	0.207	0.05			
(8)	O	0.5	0.293	0.280	0.04			
(9)	O	0.5	0.294	0.580	0.05			
(10)	O	1.0	0.080	0.770	0.05			
(11)	O	1.0	0.367	0.860	0.05			

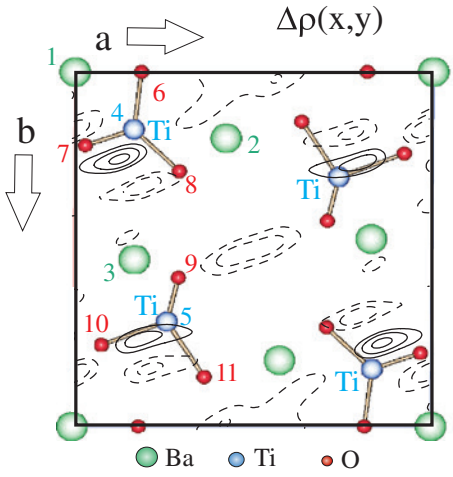

Fig. 3: Difference electron density contour plot Δρ (x, y), calculated after refinement of the barium positions. The positive peaks (solid lines) indicate the approximate positions of the titanium atoms (blue). For comparison the fully refined structure model is superimposed. Labels 1–11 correspond to atoms listed in Table 1.

symmetrically equivalent ones given by primed numbers. Also, the weak peak (D) is attributable to the vector between O(8) and O(8'). Although the study of P(u, v) is helpful to set up a structure model, we emphasize that this discussion needs a caveat, since in the structure many nearby interatomic vectors also exist and a quantitative interpretation in terms of peak height is limited. For instance with regard to peak (A) a similar interatomic vector between Ti(4) and Ti(5) (not drawn) exists, which is expected to contribute. Similarly, peak (C) is also close to the Ba(1)–Ti(4) and Ba(3)–Ti(5) interatomic vectors. In addition, care has to be taken in the analysis of P(u, v) as truncation errors are important due to the limited data set. Nevertheless the correlations are sufficient to set up a preliminary structure model including only the barium atoms Ba(1), Ba(2) and Ba(3).

Refinement of the barium coordinates yields an unweighted residuum of 30% [16, 18]. Once the positions of the heavy atoms are approximately known, it can be assumed that the calculated scattering phases [α_{calc} (hk)] based on the barium positions only approximately correspond to the experimental ones [α_{obs} (hk)] corresponding to the complete structure. In the present case of a z-projected structure which is centrosymmetric owing to the *p2* plane group symmetry and its two-dimensionality, the determination of the scattering phase is reduced to the determination of the sign of the structure factor amplitude, i.e. F_{obs} (hk) = | F_{obs} (hk)| × exp[iα_{calc} (hk)] = ± |F_{obs} (hk)|. This means that F_{obs} (hk) is a real number with α_{calc} (hk) either 0 or π.

The remaining part of the structure can subsequently be derived by calculating the difference charge density [$\Delta\rho$ (x, y)] which is given by the FT of the difference between the observed and the calculated structure factor using α_{calc} (hk) as phases: $\Delta\rho(x, y) = \sum(|F_{obs}(hk)| - |F_{calc}(hk)|) \times \exp[i\alpha_{calc}(hk)] \times \exp[-i2\pi(hx + ky)]$, where the summation runs over all reflections with indices (hk).

The calculated difference charge density is shown in Figure 3 with the refined atomic positions of all atoms within the unit cell superimposed. It can be seen that the positive peaks in $\Delta\rho$ (x, y) very well indicate the positions of the so far not considered titanium atoms. Refinement of the atomic positions including barium and titanium yields R_U = 18%, which can be interpreted as that the gross features of the structure are well modeled, i.e. the condition α_{calc} (hk) = α_{obs} (hk) is met for almost all reflections. This allows the calculation of the charge density, $\rho(x, y)$, by FT of F_{obs} (hk) again using α_{calc} (hk) now derived from the refined positions of both, barium and titanium: $\rho(x, y) = \sum|F_{obs}(hk)| \times \exp[i\alpha_{calc}(hk)] \times \exp[-i2\pi(hx + ky)]$.

This directly provides a charge density image of the structure which is shown in Figure 4 together with the refined positions of all atoms. It can be seen that for all atoms in the unit cell there is a corresponding charge density. Again, some disagreement between the atomic positions and the peak locations exists which is due to truncation errors resulting from the finite Fourier summation. Figure 5 shows for all reflections the relation between |F_{obs} (hk)| and |F_{calc} (hk)|. The dashed line corresponds to the condition |F_{obs} (hk)| = | F_{calc} (hk)|. The numerical

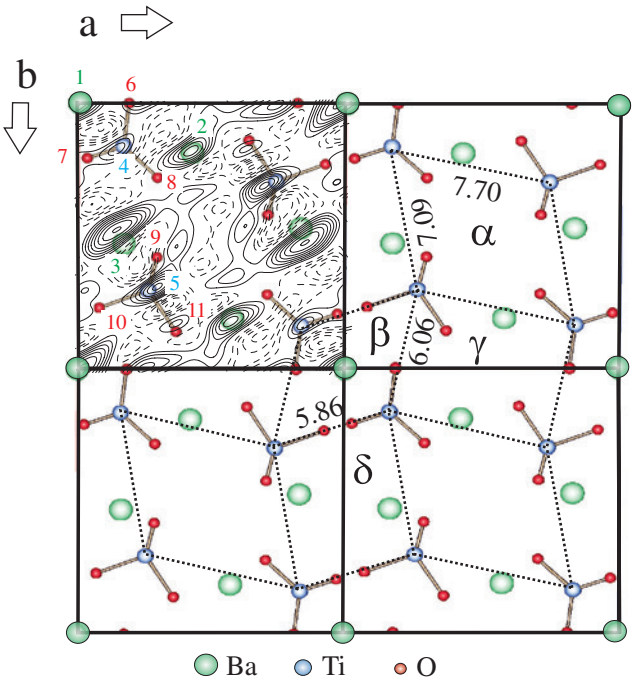

Fig. 4: (a): Calculated electron density contour plot, ρ (x, y). For comparison the fully refined structure model is superimposed. Some deviations between refined atomic positions and the charge density peaks are due to truncation errors. Four unit cells are shown to emphasize the tiling. Labels 1–11 correspond to atoms listed in Table 1. Different tiling elements are labeled by $\alpha, \beta, \gamma, \delta$. Numbers are distances in Ångstrøm units.

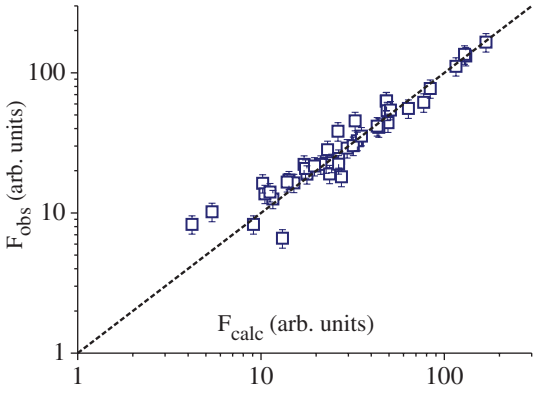

Fig. 5: Plot of $|F_{obs}(hk)|$ versus $|F_{calc}(hk)|$ for all 43 reflections of the data set on a logarithmic scale. The dashed line corresponds to the condition $|F_{obs}(hk)| = |F_{calc}(hk)|$. For the numerical data we refer to Table 2. Error bars refer to the average systematic error only. No weighting scheme was used for the refinement.

data are given in Table 2. The agreement between them (R_U=14%) can be viewed as very good given the overall low intensity of the reflections. Some larger discrepancies are only observed for a few very weak reflections [(01), (11) and (16)] which could hardly be discriminated from the background and are associated with a statistical error larger than 50%. Note, that no weighting scheme was used for the refinement. Error bars shown in Figure 5 refer to the average systematic error only.

In Figure 4 four unit cells are shown for the refined structure model emphasizing the tiling. There are two types of double triangles (α and β) as well as two types of slightly distorted rectangles (γ and δ). In the center of

Tab. 2: Comparison between observed and calculated structure factor amplitudes obtained for the best fit. The parameter α_{calc} (hk) is the calculated scattering phase.

h	k	$\|F_{obs}(hk)\|$	$\|F_{calc}(hk)\|$	α_{calc} (hk)
0	1	6.6	13.1	0
0	4	77.3	83.9	0
0	5	12.6	11.6	0
0	6	61.5	77.2	0
0	8	45.4	32.6	π
1	1	10.2	5.4	0
1	2	62.9	48.2	0
1	3	22.6	22.7	π
1	4	165.5	168.9	0
1	5	17.2	14.2	π
1	6	16.3	10.2	π
1	7	28.3	23.1	π
1	8	16.4	15.1	0
2	0	32.7	33.6	0
2	1	44.1	49.3	0
2	2	18.1	27.5	0
2	3	55.7	63.7	π
2	4	24.5	26.5	0
2	6	22.8	24.3	0
2	7	63.1	48.4	π
2	8	22.2	21.2	π
3	0	8.3	4.2	π
3	1	13.7	10.5	π
3	2	40.8	43.9	π
3	3	131.8	131.1	0
3	4	16.6	13.9	π
3	5	53.6	48.8	0
3	7	29.0	29.5	π
3	8	22.2	17.2	π
4	0	30.2	31.9	π
4	1	111.3	115.9	0
4	2	14.1	11.2	π
4	3	135.5	129.1	0
4	5	18.9	17.8	π
4	6	20.8	17.5	π
4	7	54.3	50.9	0
5	3	38.3	26.3	π
5	4	19.0	23.7	0
5	5	41.6	43.1	0
6	4	21.6	19.6	π
6	6	22.3	26.5	0
6	7	8.3	9.1	0
7	2	35.4	35.3	π

the smaller double triangle (α) one barium atom is located whereas all other barium atoms are located approximately at two out of four edges of the rectangles (γ, δ). The lengths of the edges of the tiling elements vary between 7.70 Å (maximum) and 6.06 Å (minimum) as labeled. Titanium atoms are coordinated by three oxygen atoms approximately forming a triangle. The average (projected) Ti–O distance is equal to 2.14 Å, which is a bond length typically seen in titanium oxides. The shortest one (1.64 Å) is between Ti(5) and O(9), while the longest one (2.53 Å) is between Ti(5) and O(10). It should be kept in mind, however, that he refinement of the oxygen positions is the least accurate one. We estimate the uncertainty for the Ti–O distance determination to lie in the 0.1–0.2 Å range. There is no significant vertical corrugation within the structure. The measurement of the diffraction rods, i.e. along the continuous ℓ coordinate indicated an almost flat structure. In view of the limited data set and access in k-space we did not try to refine the individual z-positions of the atoms.

We have allowed for the refinement of the atomic disorder and the occupancy factors. Atomic disorder is taken into account by the generalized atomic displacement factor (T_{hk}) which is given by: $T_{hk} = \exp[-2\pi^2 \sum\sum U_{ij} a^*_i a^*_j h_i h_k]$, where the U_{ij} represent the mean squared displacement amplitudes, the a^*_i the lengths of the reciprocal unit vectors. The (double) summation runs over i, j = (1, 2) corresponding to $h_1 = h$ and $h_2 = k$. For details, see for instance Ref. [19]). In the isotropic approximation very large values in the range between $U_{11} = U_{22} = U_{iso} = 0.05 - 0.27$ Å^2 are found (see Table 1). Most importantly, the fit quality is improved if for the Ba atoms (1) and (3) anisotropic disorder is taken into account. For Ba(3) we obtain $U_{11} = 0.67 \pm 0.10$ Å^2, $U_{22} = 0.40 \pm 0.10$ Å^2 and $U_{12} = -0.28 \pm 0.09$ Å^2, the latter representing the orientation of the tensor ellipse relative to the lattice vectors [for Ba(1) the fit result is: $U_{11} = 0.88 \pm 0.23$ Å^2, $U_{22} = 0.65 \pm 0.18$ Å^2, $U_{12} = -0.57 \pm 0.20$ Å^2]. These huge values are only explainable by a model in which the position of the Ba atoms are split by several tenths of an Ångstrøm over different sites. We attribute this to the modulation of the Ba positions similar to the modulation of the Ti atoms visible in the STM image in Figure 1c. As for the SXRD analysis we use the projection of the large modulated unit cell [transformation matrix $M = a_{11} = 27$; $a_{21} = 10$; $a_{21} = 3$; $a_{22} = 20$] into the 20 times smaller one [$M = a_{11} = 27/5$; $a_{21} = 2$; $a_{21} = 3/4$; $a_{22} = 5$], the U_{ij} represent the "blurring" of the atomic positions. Notably, the consideration of the component $U_{12} \neq 0$ is very important for obtaining a good fit, indicating the 32° angle between the a-axis of the unit cell and the modulation direction. Consideration of anisotropic atomic displacements improved the fit only in the case of Ba atoms (1) and (3), which contribute most strongly to the scattering amplitude.

Secondly, the occupancy factors (Θ) of the individual sites were varied. We find that the occupancy of the barium site (2) as well as of the oxygen sites (8) and (9) are equal to $\Theta = 0.5$ with an estimated uncertainty of about 0.15–0.25 for the barium and the oxygen sites, respectively. This reflects the presence of (random) vacancies. Taking this into account the stoichiometry corresponds to $Ba_4Ti_4O_{10}$ rather than $Ba_5Ti_4O_{12}$ in the case of full occupancy of all sites. The oxygen deficient stoichiometry relative to barium titanate ($Ba_4Ti_4O_{12}$) is related to the reducing preparation conditions (annealing under UHV conditions) of the film and the observation of Ti^{3+} species in X-ray photoemission spectra [7].

In summary, we have carried out a surface X-ray structure analysis of the approximant of the two-dimensional $BaTiO_3$ related oxidic quasicrystal. We find that the building block composing the $3^2.4.3.4$ Archimedean tiling is formed by titanium atoms which have previously been observed in scanning tunneling microscopy images. This structure has been described by J. Kepler almost 400 years ago and thus can be viewed as the oldest complex surface structure in history. Titanium atoms are threefold coordinated by oxygen atoms separated by barium atoms. Due to the close resemblance of the approximant with the quasicrystal this study is an important step into the direction to completely solve the OQC's structure and the understanding of its formation and stability.

Acknowledgment: This work is supported by the Deutsche Forschungsgemeinschaft through Sonderforschungsbereich SFB 762 (Funktionalität oxidischer Grenzflächen). We thank Frank Weiss and Ralf Kulla for technical support. We also thank the staff of the ESRF for their hospitality and help during the experiments.

References

[1] D. Shechtman, I. Blech, D. Gratias, J. W. Cahn, Metallic phase with long-range orientational order and no translational symmetry. *Phys. Rev. Lett.* **1984**, *53*, 1951.
[2] W. Steurer, S. Deloudi, Crystallography of Quasicrystals, Springer Verlag, Heidelberg, Dordrecht, London and New York 2009.
[3] N. Wang, H. Chen, K. H. Kuo, Two-dimensional quasicrystal with eightfold rotational symmetry. *Phys. Rev. Lett.* **1987**, *59*, 1010.
[4] X. Zeng, G. Ungar, Y. Liu, V. Percec, A. E. Dulcey, J. K. Hobbs, Supramolecular dendritic liquid quasicrystals. *Nature* **2004**, *428*, 157.
[5] J. Mikhael, J. Roth, L. Helden, C. Bechinger, Archimedean-like tiling on decagonal quasicrystalline surfaces. *Nature* **2008**, *454*, 501.

[6] S. Fischer, A. Exner, K. Zielske, J. Perlich, S. Deloudi, W. Steurer, P. Lindner, S. Förster, Colloidal quasicrystals with 12-fold and 18-fold diffraction symmetry. *Proc. Natl. Acad. Sci.* **2011**, *108*, 1810.
[7] S. Förster, K. Meinel, R. Hammer, M. Trautmann, W. Widdra, Quasicrystalline structure formation in a classical crystalline thin-film system. *Nature* **2013**, *502*, 215.
[8] A. I. Goldman, R. F. Kelton, Quasicrystals and crystalline approximants. *Rev. Mod. Phys.* **1993**, *65*, 213.
[9] J. Kepler, Harmonices Mundi, Linz (1619).
[10] B. Grünbaum, G. C. Shepard, Tilings by regular polygons. *Math. Magazine* **1977**, *50*, 227.
[11] S. Förster, M. Trautmann, S. Roy, W. A. Adeagbo, E. M. Zollner, R. Hammer, F. O. Schumann, S. Meinel, S. K. Nayak, K. Mohseni, W. Hergert, H. L. Meyerheim, W. Widdra, Observation and strcuture determination of an oxide quasicrystal approximant. *Phys. Rev. Lett.* **2016**, *117*, 095501.
[12] P. A. Stampfli, Dodecagonal quasi-periodic lattice in two dimensions. *Helv. Phys. Acta* **1986**, *59, 1260*.
[13] F. Gähler, Quasicrystalline Materials (Eds. C. Janot, J. M. Dubois) World Scientific, Singapore, p. 272, 1988.
[14] E. Cockayne, M. Mihalkovic, C. L. Henley, Structure of periodic crystals and quasicrystals in ultrathin films of Ba-Ti-O. *Phys. Rev. B* **2016**, *93*, 020101(R).
[15] I. K. Robinson, Crystal truncation rods and surface roughness. *Phys. Rev. B* **1986**, *33*, 3830.
[16] The unweighted residual (R_u) is defined as: $R_u = \sum||F_{obs}|-|F_{calc}|| / \sum|F_{obs}|$. The summation runs over all datapoints.
[17] M. J. Buerger, Kristallographie, Walter de Gryuter Verlag, Berlin and New York 1977.
[18] U. H. Zucker, E. Perenthaler, W. F. Kuhs, R. Bachmann, H. Schulz, PROMETHEUS. A program system for investigation of anharmonic thermal vibrations in crystals. *J. Appl. Crystallogr.* **1983**, *16*, 358.
[19] F. W. Kuhs, Generalized atomic displacements in crystallographic structure analysis. *Acta Cryst.* **1992**, *A48*, 80.